11.9 CHANGES IN CIRRUS CLOUDINESS AND THEIR RELATIONSHIP TO CONTRAILS

Patrick Minnis
Atmospheric Sciences, NASA Langley Research Center, Hampton, VA 23681

J. Kirk Ayers, Rabindra Palikonda, David R. Doelling,
AS&M, Inc., Hampton, VA 23666

Ulrich Schumann, Klaus Gierens
DLR, Oberpfaffenhofen, Germany

1. INTRODUCTION

Condensation trails, or contrails, formed in the wake of high-altitude aircraft have long been suspected of causing the formation of additional cirrus cloud cover. More cirrus is possible because 10 - 20% of the atmosphere at typical commercial flight altitudes is clear but ice-saturated (e.g. Gierens et al. 1999). Since they can affect the radiation budget like natural cirrus clouds of equivalent optical depth and microphysical properties (e. g. Meerkötter et al. 1999), contrail-generated cirrus clouds are another potential source of anthropogenic influence on climate. Initial estimates of contrail radiative forcing (CRF) were based on linear contrail coverage and optical depths derived from a limited number of satellite observations (Minnis et al. 1999). Assuming that such estimates are accurate, they can be considered as the minimum possible CRF because contrails often develop into cirrus clouds unrecognizable as contrails (e.g., Minnis et al. 1998). These anthropogenic cirrus are not likely to be identified as contrails from satellites and would, therefore, not contribute to estimates of contrail coverage. The mean lifetime and coverage of spreading contrails relative to linear contrails are needed to fully assess the climatic effect of contrails, but are difficult to measure directly. However, the maximum possible impact can be estimated using the relative trends in cirrus coverage over regions with and without air traffic.

In this paper, the upper bound of CRF is derived by first computing the change in cirrus coverage over areas with heavy air traffic relative to that over the remainder of the globe assuming that the difference between the two trends is due solely to contrails. This difference is normalized to the corresponding linear contrail coverage for the same regions to obtain an average spreading factor. The maximum contrail-cirrus coverage, estimated as the product of the spreading factor and the linear contrail coverage, is then used in the radiative model of Minnis et al. (1999) to estimate the maximum potential CRF for current air traffic.

*Corresponding author address: Patrick Minnis, NASA Langley Research Center, MS 420, Hampton, VA 23681-2199. email: p.minnis@larc.nasa.gov.

2. DATA

Mean annual cirrus frequency and amount and total cloud amount were computed on a 3° x 3° latitude-longitude grid using the daytime surface and ship observations collected and screened by Hahn and Warren (1999) between 70°N and 70°S. Several categories were used to classify each region at some level of expected contrail coverage. A set of land air traffic regions (ATRs) were defined for the United States of America (USA; 30°N - 50°N; 50°W - 130°W), central Europe (EUR; 40°N - 60°N, 10°W - 15°E); western Asia (WA; 35°N - 75°N, 90°E 0 180°E). The remaining land areas constitute the land non-air traffic regions (NATR). Similarly, ocean ATRs were defined for the North Atlantic (NA; 35°N - 70°N, 70°W - 20°E) and North Pacific (NP; 30°N - 70°N, 120°E - 110°W). An ocean NATR was defined to include the remainder of the ocean regions. These large regions provide a means for a gross assessment of the locations of trends.

A more refined classification was made to maximize any contrail signal. All regions having a linear contrail coverage $c > 0.5\%$ from the database of Sausen et al. (1998) were designated contrail or CON regions. Those remaining are non-contrail or NCON regions. Over land (land percentage exceeding 1%), there are 201 CON and 3024 NCON regions. Over oceans, there are 31 NCON and 3944 NCON regions. The mean linear contrail coverage is 1.44% and 0.05% for the land CON and NCON regions, respectively. Corresponding contrail amounts over oceans are 0.70 and 0.02%. The NCON regions were further subdivided in two sets using $c = 0.02\%$ to divide them. Mean annual seasonal cirrus and total cloud amounts were computed for each classification using only those 3° regions having surface data for more than 80% of the period. Linear least squares regressions were used to compute the regional cirrus and total cloud cover trend for the period.

Similarly, high cloud cover from the International Satellite Cloud Climatology Project (ISCCP; Rossow and Schiffer 1999) 1984-1994 D2 dataset and the 1989 -1999 High-Resolution Infrared Radiation Sounder (HIRS; Wylie and Menzel 1999) data were averaged in the same manner as the surface observations to compute trends. Data taken between July 1991 and July 1993 were not used because of contamination of the satellite signal by the Mt. Pinatubo eruption.

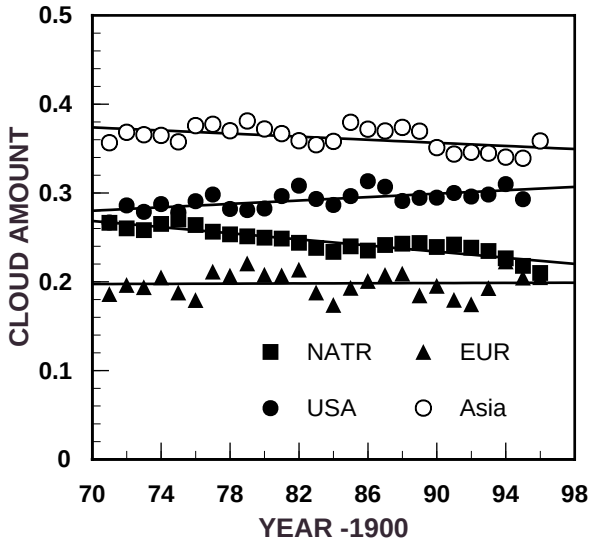

Fig. 1. Trends in mean cirrus coverage over land from surface observations.

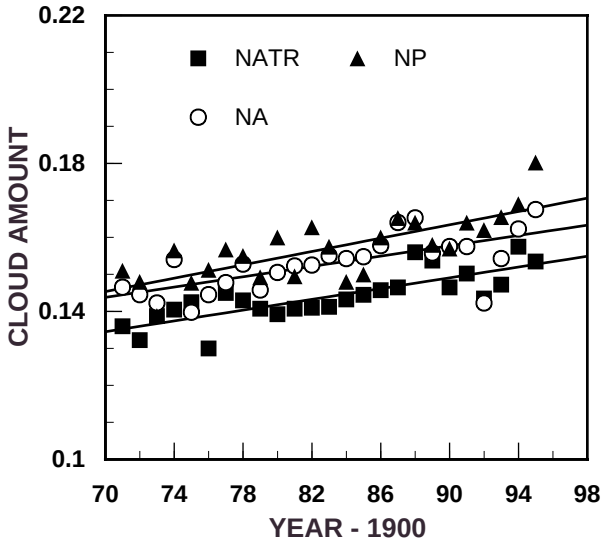

Fig. 2. Trends in mean cirrus coverage over ocean from surface observations.

3. RESULTS

Figure 1 shows the trends in mean annual cirrus coverage over land areas between 1971 and 1996 from surface observations. The data end in 1995 over the USA because the number of samples was half of that in previous years. The cirrus cloud amount increased over the USA, remained steady over EUR, and decreased over WA and the NATR. The trends for the period are summarized in Table 1 for the surface, HIRS, and ISCCP observations. The relative trends are generally consistent for all of the datasets although they do not cover all of the same years. All of the ATR trends exceed the NATR trends. On average, the differences are greatest over the USA with a 2.9%/dec increase in cirrus cloudiness relative to the NATR. The average relative trends over WA and EUR are 1.0 and 2.7 %/dec. The surface-based total cloud amounts changed at 1.3, -0.2, -0.9, and 2.6%/dec over the USA, EUR, WA, and the NATR respectively. Thus, over the land ATRs, the cirrus trends account for almost all of the change in total cloud cover. Total cloudiness increased over the NATRs, apparently due a substantial rise in low and midlevel cloudiness. Although such increases would tend to hinder the observation of high clouds, the technique used by Hahn and Warren (1999) assumes that the same amount of high cloudiness is present in both obscured and unobscured conditions. Thus, the decrease of NATR cirrus coverage observed in Fig. 1 should reflect the actual changes. The relative cirrus trends from the USA and EUR surface data are statistically significant at the 99% confidence level.

Table 1. Trend in cirrus coverage, %/decade.

Land	Surface	HIRS	ISCCP
WA	-0.9	2.2	2.7
EUR	0.1	5.2	3.9
USA	1.0	3.9	4.9
NATR	-1.7	1.0	1.7
Ocean			
NA	0.7	4.1	1.0
NP	0.9	2.1	1.7
NATR	0.7	2.9	1.4

The ocean cirrus data in Fig. 2 show an increase everywhere. Since the slopes of the trend lines in Table 1 are not statistically different, there is no differentiating signal apparent for these broad marine areas. Mean total cloud amount changed by 0.0, 0.8, and 1.2%/dec over the NA, NP, and marine NATR over the same period suggesting that lower clouds decreased over the NA and increased over the NATR. The satellite-based trends in Table 1 for ocean are consistent with the surface results in that they are positive with no significant differences among the regions. Overall, the surface data show cirrus cover changing at -1.2, 0.7, and 0.1%/dec over land, ocean, and all regions, respectively. Correspondingly, total cloudiness changes by 1.6, 0.7, and 1.0%/dec. Both satellite datasets show a general increase in global cirrus amount.

Cirrus frequency increased at a faster rate over the USA than cirrus coverage indicating a decrease in the amount when present. The frequency over EUR did not change. Cirrus frequency decreased at a greater rate than the amount over WA and NATR. Cirrus frequency of occurrence increased at faster rate over all ocean areas than the cirrus amount.

Because the USA and EUR have the heaviest air traffic, it is expected that a contrail-related signal would be greatest in those areas. Previous studies have indicated that contrail amount or occurrence vary seasonally. Thus, any contrail-related trends in cirrus

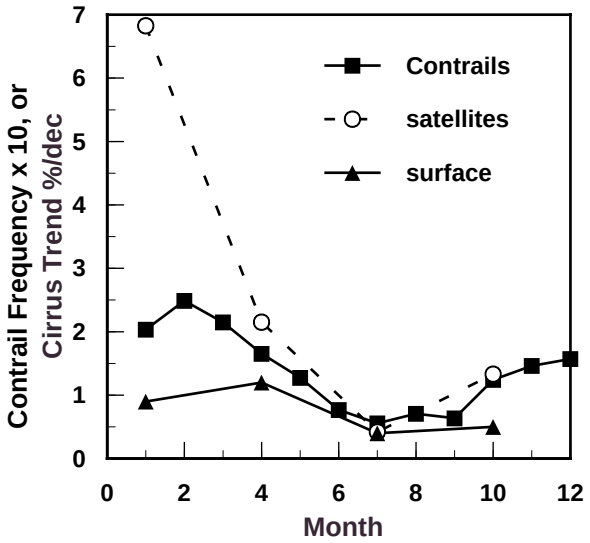

Fig. 3. Seasonal variation in persistent contrail occurrence and trends in cirrus coverage from the surface and from HIRS and ISCCP (satellites).

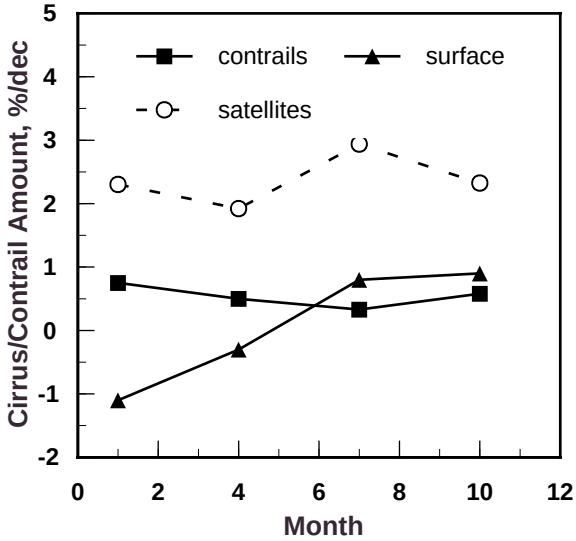

Fig. 4. Seasonal variation of linear contrail coverage and trends in cirrus coverage from the surface and from HIRS and ISCCP (satellites).

should have similar seasonal cycles. Figure 3 shows the mean seasonal trends in cirrus amounts over the USA with the monthly persistent contrail occurrence frequency from surface observations taken during 1993-94 and 1998-99 at US Air Force bases (Minnis et al. 1997). Persistent contrails occur most frequently during winter and early spring over the USA and least often during summer. According to surface observers, cirrus cloudiness has been increasing most rapidly during winter and spring and most slowly during summer and fall. The satellite trends (averages of HIRS and ISCCP) indicate a strong peak during winter with a distinct summer minimum. From Fig. 3, it can be concluded that the seasonal cycle in cirrus trends is very consistent with the seasonal variation of contrails over the USA.

The seasonal mean linear contrail coverage derived from a year of 1-km satellite data over Europe (Mannstein et al. 1999) are plotted in Fig. 4 with the corresponding cirrus trends from the surface and satellites. The surface observations yield a drop in cirrus during winter and spring with increases during the other seasons. All of the seasonal trends are positive from the satellite data and relatively consistent with the surface data except during winter. However, the maximum trend occurs during the summer when the minimum contrail coverage is recorded. The general consistency of the trends and contrails over the USA suggests a strong link between the quantities, but such is not the case over Europe. Thus, the apparent link over the USA may be coincidental or other changes in cloudiness occurred over Europe that mask a seasonal contrail-cirrus effect. Even in the absence of spreading, a trend in cirrus equivalent to the satellite-observed linear contrails should be expected because those are clouds that would not have formed otherwise. Given the trends in cirrus over the land NATR, it appears that some other factors are affecting the cirrus over land globally. If the EUR seasonal trends are normalized to the NATR trends, then all of them become positive and nearly equal to the satellite values except during winter.

Table 2. Trends in land cirrus coverage, %/decade.

Contrail	Surface	HIRS	ISCCP
24°N - 60°			
≥ 0.5%	0.0	4.6	4.5
0.02 - 0.5%	-1.3	2.5	3.6
< 0.02%	-1.7	-0.4	2.2
Global			
≥ 0.5%	0.0	4.4	4.3
0.02 - 0.5%	-1.8	2.7	2.1
< 0.02%	-1.7	-1.8	0.9

The trends in cirrus coverage over land CON and NCON regions are summarized in Table 1 for the northern midlatitudes and for all considered regions. The mean CON trends are different from both of the NCON categories at the 99% confidence level for all of the datasets. The relative trend differences between the CON and NCON regions range from 1. 7% - 4.8%/dec between 24 and 60°N and from 1.8% and 6.4% globally. Because many of the CON regions are in the USA and EUR, the trends are similar to but greater than those in Table 1. No significant differences were found between the CON and NCON trends over ocean from the surface data. The combined land and ocean results yield trend differences 0.4 and 2.6%/dec from surface and ISCCP data, respectively.

To determine the spreading factor, it is assumed that the differences between the CON and NCON trends represent the contrail-induced cloud cover. Using the

24-60°N surface data over land, the CON cirrus coverage has increased by 5.1% over the past 30 years. The corresponding difference between the CON and NCON mean linear contrail coverage for the mid-1990s is 1.3%. Thus, the spreading factor would be 3.9 (3.7 globally). If the mean satellite results were used, the spreading factor would be more than twice that from the surface. If all of the data were used over land and ocean, the spreading factor from the surface and ISCCP data would be ~ 1.0 and up to 5.8 for the satellite data.

Because of the record length and fixed stations, the land surface data should provide the most statistically reliable trends for estimating spreading. Although the satellite data are more objective, they only cover a maximum of 9 years and have some temporal sampling and calibration issues that need further study. Additionally, the NCON trends computed for the northern midlatitudes are probably more representative of the background conditions for most air traffic. Thus, a spreading factor of 3.9 is adopted as the best guess for computing the upper limit for contrail-induced cirrus cloudiness. Multiplying the 0.087% mean linear contrail coverage of Sausen et al. (1998) by this factor yields an estimate of 0.34% maximum increase in cirrus coverage as a result of contrail formation and spreading.

Using the approach of Minnis et al. (1999), with contrails having a 0.3 optical depth and a 24-µm effective particle diameter, yields a global, net top-of-atmosphere radiative forcing of 0.066 Wm^{-2}. Rind et al. (2000) used an optical depth of 0.33 when they simulated contrails in an interactive-ocean general circulation model (GCM) by adding cirrus cover to the atmosphere in various increments and horizontal distributions. They found a relatively linear response between the additional cloudiness and the surface and atmospheric temperatures for the resulting equilibrium states. A surface temperature increase of 0.3°C resulted from a high-cloud cover change of 0.4%. The change corresponding to the current estimate of maximum contrail-cirrus coverage was computed by linearly scaling the model result to 0.34% and accounting for the optical depth differences. The resulting value of 0.234°C represents the global surface air temperature change for the *maximum* expected change in cirrus due to current air traffic compared to an equilibrium value of 0.086°C estimated by Rind et al. (2000) for current linear contrail coverage. From the model results, the tropospheric temperature should also increase by ~0.4°C for the estimated maximum coverage.

4. CONCLUDING REMARKS

It can be concluded that air traffic is causing an increase in cloud cover. Despite the differences in perspective, methodology, and sampling, the satellite and surface observations all show a statistically significant increase in cirrus coverage over areas where air traffic is heaviest relative to other regions. The mechanisms for such increases are well documented. However, many uncertainties in contrail properties and natural cloud variability must still be addressed to more accurately compute the range of expected impacts from contrail-induced cloudiness. A more concerted effort is needed to develop reliable statistics of contrail growth, optical depths, and lifetimes as functions of aircraft, temperature, and meteorological conditions. Longer time series of cirrus coverage from well-calibrated consistent satellite data will also help refine the observational estimates of contrail impacts. Contrails only form when the conditions are suitable and aircraft are present. Furthermore, the addition of contrail cirrus to the atmosphere is a gradually increasing process, so that equilibrium conditions are unlikely to occur in the near future. Thus, more realistic simulations of contrails in GCMs are also required. A combination of improved models and measurements should enable a reasonably accurate determination of climatic effects of future air traffic.

REFERENCES

Gierens, K., U. Schumann, M. Helten, H. Smit, and A. Marenco, 1999: A distribution law for relative humidity in the upper troposphere and lower stratosphere derived from three years of MOZAIC measurements, *Ann. Geophysicae*, **17**, 1218-1226.

Hahn, C. J., and S. G. Warren, 1999: *Extended Edited Synoptic Cloud Reports from Ships and Land Stations Over the Globe, 1952-1996.* NDP026C, Carbon Dioxide Information Analysis Center, Oak Ridge National Laboratory, OAK Ridge, TN.

Mannstein, H., R. Meyer, and P. Wendling, Operational detection of contrails from NOAA-AVHRR-data. *Int. J. Remote Sensing.,* 20, 1641-1660, 1999.

Meerkötter, R., U. Schumann, D. R. Doelling, P. Minnis, T. Nakajima, and Y. Tsushima, 1999: Radiative forcing by contrails. *Ann. Geophys.*, **17**, 1070-1084.

Minnis, P. J. K. Ayers, and S. P. Weaver, 1997: Surface-Based Observations of Contrail Occurrence Frequency Over the U.S., April 1993 - April 1994. *NASA RP 1404*, 81 pp.

Minnis, P., U. Schumann, D. R. Doelling, K. M. Gierens, and D. W. Fahey, 1999: Global distribution of contrail radiative forcing. *Geophys. Res. Ltrs.*, **26**, 1853-1856.

Minnis, P., D. F. Young, L. Nguyen, D. P Garber,. W. L. Smith, Jr., and R. Palikonda, 1998: Transformation of contrails into cirrus during SUCCESS. *Geophys. Res. Ltrs.*, **25**, 1157-1160.

Rind, D., P. Lonergan, and K. Shah, 2000: Modeled impact of cirrus cloud increases along aircraft flight paths. *J. Geophys. Res.*, **105**, 19,927-19,940.

Rossow, W. B. and R. A. Schiffer, 1999: Advances in understanding clouds from ISCCP. *Bull Am. Meteor. Soc.*, **80**, 2261-2287.

Sausen, R., K. Gierens, M. Ponater, and U. Schumann, 1998: A diagnostic study of the global coverage by contrails, Part I: Present day climate. *Theor. Appl. Climatol.*, **61**, 127-141.

Wylie, D. P. and W. P. Menzel, 1999: Eight years of high cloud statistics using HIRS.*J. Climate*, **12**, 170-184.